Mechanisms of Climate Change in the Semiarid African Sahel: The Local View

ALESSANDRA GIANNINI

International Research Institute for Climate and Society, The Earth Institute at Columbia University, Palisades, New York

(Manuscript received 6 March 2009, in final form 4 August 2009)

ABSTRACT

Application of the moist static energy framework to analyses of vertical stability and net energy in the Sahel sheds light on the divergence of projections of climate change. Two distinct mechanisms are sketched. In one, anthropogenic warming changes continental climate indirectly: warming of the oceans increases moist static energy at upper levels, affecting vertical stability globally, from the top down, and driving drying over the Sahel, in a way analogous to the impact of El Niño–Southern Oscillation on the global tropical atmosphere. In the other, the increase in anthropogenic greenhouse gases drives a direct continental change: the increase in net terrestrial radiation at the surface increases evaporation, favoring vertical instability and near-surface convergence from the bottom up.

In both cases the surface warms, but in the first precipitation and evaporation decrease, while in the second they increase. In the first case, land surface warming is brought about by the remotely forced decrease in precipitation and consequent decrease in evaporation and increase in net solar radiation at the surface. In the second, it is brought about by the increase in net terrestrial radiation at the surface, amplified by the water vapor feedback associated with an increase in near-surface humidity.

1. Introduction

Global warming, as manifested in the increase in global-mean near-surface temperature, is expected to lead to increased evaporation over land. In the absence of credible regional rainfall projections it is often argued that such change in itself could lead to water stress, adversely impacting dryland ecosystems and the services they provide (Adeel et al. 2005). However, in tropical dry lands these systems have historically been dominated by variability in rainfall, not in temperature.

Here I seek to make sense of temperature and rainfall changes as one. I use the African Sahel, a semiarid region at the margin of influence of the Northern Hemisphere summer monsoon, as a case study. Based on the general expectation of global warming leading to an intensification of the hydrological cycle—with climatologically wet regions becoming wetter, dry regions becoming drier, and rainfall events becoming more intense (Trenberth et al. 2003; Neelin et al. 2003; Meehl et al. 2007b)—one would expect a drier future Sahel since this is a climatologically dry region with annual rainfall totaling 200–600 mm. However, projections of twenty-first-century change are most uncertain (Biasutti and Giannini 2006; Cook and Vizy 2006; Douville et al. 2006; Christensen et al. 2007), with equal numbers of models predicting significantly wetter or drier future or no significant change with respect to present conditions.

Recent research with atmospheric models forced by the long-term history of global sea surface temperature (SST) supports the claim of a controlling role for the oceans on the climate of the Sahel (Giannini et al. 2003; Bader and Latif 2003; Lu and Delworth 2005; Hoerling et al. 2006; Folland et al. 1986). Warming of the tropical oceans is a nonnegligible component of historical Sahel drought (e.g., Hagos and Cook 2008; Ting et al. 2009). If carried forward, the inescapable conclusion is one of continued drying of the Sahel since the warming of the oceans (Levitus et al. 2000; Barnett et al. 2005) is projected to continue. However, rainfall has partially recovered since the driest mid-1980s. In the Ting et al. (2009) framework—which separates an externally forced signal, with warming inducing drying from internal variability, oscillating between dry and wet states—the present recovery can be attributed to the interference of

Corresponding author address: Alessandra Giannini, International Research Institute for Climate and Society, The Earth Institute at Columbia University, Palisades, NY 10964.
E-mail: alesall@iri.columbia.edu

DOI: 10.1175/2009JCLI3123.1

internal variability in the Atlantic Ocean (Ting et al. 2009; Knight et al. 2006; Hoerling et al. 2006) with the global warming signal: Atlantic sea surface temperatures strengthened the drying induced by warming of the oceans when in a phase that favored a southward location of the intertropical convergence zone, in the 1970s and 1980s, but are now in a configuration favorable for Sahel rainfall; hence, they are partially counteracting the drying trend associated with global warming.

In the context of the oceans controlling the climate of the Sahel it is reasonable to ask whether it is differences in patterns of SST change that can explain the differences in sign of projection of future regional rainfall change. Biasutti et al. (2008) show that this does not seem to be the case: a reconstruction of Sahel rainfall based on a linear regression of the SST indices that explain twentieth-century behavior—an Indo-Pacific index and an index of the meridional gradient in the Atlantic—fails to account for the divergence among models in twenty-first century projections.

Section 3 will show that the spatial patterns of SST change simulated at the end of the twentieth and twenty-first centuries in the Coupled Model Intercomparison Project phase 3 (CMIP3) models,[1] especially in the tropics (30°S–30°N), cannot explain the divergence in projections of Sahel rainfall. Consequently, the remainder of the paper considers an alternative working hypothesis. Can the divergence of climate models in projections of future rainfall change in the Sahel, exemplary of future change in other semiarid margins of monsoons, be explained by differences in the response of the land surface directly related to the local interaction of precipitation, evaporation, and anthropogenic influence on radiative forcing at the surface?

Liepert et al. (2004) first brought attention to the net surface energy balance as the crucial element to understanding of a changing global water cycle—the water cycle can spin down even in a warming world, for example when an increase in sulfate aerosol concentrations reduces the net solar radiation reaching the surface, hence evaporation.

Two alternative pathways are suggested that bring about change locally to the Sahel (Giannini et al. 2008). In one, the remote influence of the warming oceans drives top-down change. In analogy with the impact of the El Niño–Southern Oscillation on tropical precipitation, warming of the oceans controls vertical stability globally, bringing about a reduction in continental precipitation in those regions that cannot meet the increasing demand in energy, represented in the present analysis by near-surface moist static energy (Chiang and Sobel 2002; Chou et al. 2001; Neelin et al. 2003; Held et al. 2005). This reduction in precipitation is then reinforced by the consequent reduction in evaporation. In the other, the local response of the land surface to the anthropogenic increase in radiative forcing dominates. The increase in net terrestrial radiation at the surface drives a local increase in evaporation, which results in increased near-surface moist static energy, vertical instability, and precipitation. The increased near-surface instability and precipitation then further fuel an increase in low-level moisture convergence—a bottom-up mechanism that swamps any remote effects and results in a stronger monsoon (Haarsma et al. 2005).

Local diagnosis of these pathways focuses on the interplay between precipitation, near-surface and upper-level moist static energy, net surface and atmospheric radiation, evaporation, and surface temperature, best described by the moist static energy framework (Neelin and Held 1987). Consistently, ''local'' is taken to mean germane, or related directly to the Sahel, whereas ''remote'' means foreign, or related to factors outside of the Sahel. Otherwise stated, ''local'' goes with land driven, ''remote'' with ocean driven.

Section 2 briefly describes model output used. Section 3 reviews the role of SST in explaining twenty-first century change in Sahel rainfall. The main results of the approach taken here—a local characterization of the intersection of energy and water cycles that exploits the moist static energy framework—are presented in section 4, which is divided into three subsections. In the first, the remote, top-down and local, bottom-up mechanisms relating near-surface and upper-level vertical stability are related to precipitation change. In the second, scatterplots of regionally averaged quantities are used to diagnose changes in precipitation and temperature as they relate to changes in terms in the net surface energy budget. In the third, consistent changes in the atmospheric circulation are described as they relate to energy and water budgets. Discussion and conclusions follow.

2. Data

Model output comes from CMIP3, archived at the Program for Climate Model Diagnosis and Intercomparison (PCMDI; http://www-pcmdi.llnl.gov/) and served through the International Research Institute (IRI) Data Library (http://iridl.ldeo.columbia.edu/).

[1] The coupled ocean–atmosphere simulations made available in preparation for the Fourth Assessment Report (AR4) of the Intergovernmental Panel on Climate Change (IPCC), also known as CMIP3 of the World Climate Research Programme (WCRP). See Meehl et al. 2007a.

Output is analyzed from three types of simulations: 1) a long, that is, on the order of 500 years, *preindustrial control* (pic) simulation, in which the coupled ocean–atmosphere system is driven by forcings constant in time; 2) the *twentieth-century* (20c3m) simulations in which the system is driven by forcings that vary in time, both natural (e.g., variability in top-of-the-atmosphere insolation and volcanic eruptions) and anthropogenic (concentrations in greenhouse gases, aerosols, and in some cases land use change); and 3) *scenario A1B* (sresa1b) for the twenty-first century (Special Report on Emissions Scenarios), a ''future world of very rapid economic growth, low population growth and rapid introduction of new and more efficient technology'' (http://www.ipcc-data.org/sres/ddc_sres_emissions.html). In the following, the combination of pic and 20c3m will often be referred to as the ''historical'' simulations.

Four models are chosen using three criteria: 1) availability of a long preindustrial control simulation (condition that, alone, eliminates over half of the models in the CMIP3 archive), 2) availability of the many variables necessary for the analyses carried out here, and 3) behavior representative of the divergence in future projections of rainfall in the Sahel (based on Biasutti and Giannini 2006; see their Fig. 2b): Geophysical Fluid Dynamics Laboratory Climate Model version 2.0 (GFDL CM2.0) represents statistically significantly drier future conditions; the NCAR Community Climate System Model, version 3 (CCSM3.0) and Model for Interdisciplinary Research on Climate, medium-resolution version [MIROC(medres)] represent significantly wetter future conditions; the Centre National de Recherches Météorologiques Coupled Global Climate Model, version 3 (CNRM-CM3) represents no statistically significant change. Three of these four models are among the 10 that pass the first selection step in Cook and Vizy (2006) on the basis of their simulation of the regional climatology of rainfall. The fourth fails the test because it overestimates rainfall over the Gulf of Guinea in the eastern equatorial Atlantic. Though the number of models retained is small compared to the entire archive, the intended outcome of this study is to indirectly suggest simpler metrics that could be applied to a larger set of models.

3. Global SSTs and future rainfall change in the Sahel

As mentioned in the introduction, given that the oceans have played the dominant role in shaping the climate of the Sahel over the last century, it is reasonable to hypothesize that differences in projections of change in precipitation may be attributed to differences in SST patterns.

Figures 10 and 11 in Biasutti et al. (2008) already show that the future of Sahel rainfall cannot be reconstructed simply based on twentieth century relationships with indices of SST. Figure 1 explores differences in spatial patterns of surface air temperature between the end of the twentieth century (20c3m) and the preindustrial control (pic) on the lhs, and between the end of the twenty-first century (sresa1b) and the end of the twentieth century on the rhs. Table 1 reports correlation values of the spatial patterns of change, that is, between the lhs and rhs of Fig. 1, weighted by the cosine of latitude.

The patterns of SST change, past and future, are very similar in three out of four models, especially if one focuses on the tropics. In the plots, this is most apparent in the second and fourth rows—in models projecting no significant change in rainfall in the Sahel and a significantly wetter Sahel, respectively. The one model that deviates from this behavior is one of two models projecting a wetter future in the Sahel—that in the third row. The change in the Atlantic SST pattern in this model is consistent with the change in Sahel rainfall. At the end of the twentieth century, when the Sahel was significantly dry in this model (Biasutti and Giannini 2006), the meridional gradient was negative, with a warmer Southern Hemisphere. At the end of the twenty-first century, when the Sahel is projected to become wetter, the meridional gradient is positive. However, the Atlantic Ocean alone cannot explain the divergence in projections—the meridional gradient in the Atlantic at the end of the twenty-first century is also positive in the model predicting a drier future for the Sahel—that in the first row.

Future enhanced warming of the tropical oceans similar to that statistically associated with drought in the Sahel (Giannini et al. 2003; Ting et al. 2009) is noticeable in all models and is most consistent in the model that projects no significant future change in the Sahel—in the second row. Such a pattern is also clear in one of two models projecting a significantly wetter future—in the bottom row. These observations justify consideration of an alternative explanation, which is pursued here.

4. Relating precipitation, vertical stability, and energy in the moist static energy framework

To directly relate changes in precipitation to the thermodynamic change in radiative forcing associated with the increase in anthropogenic emissions of greenhouse gases and other pollutants, I follow the moist static energy framework—the theory developed by Neelin and Held (1987) and applied to land regions by Zeng and Neelin (1999) and Chou and Neelin (2003). Taking advantage of the fact that evaporation is part in

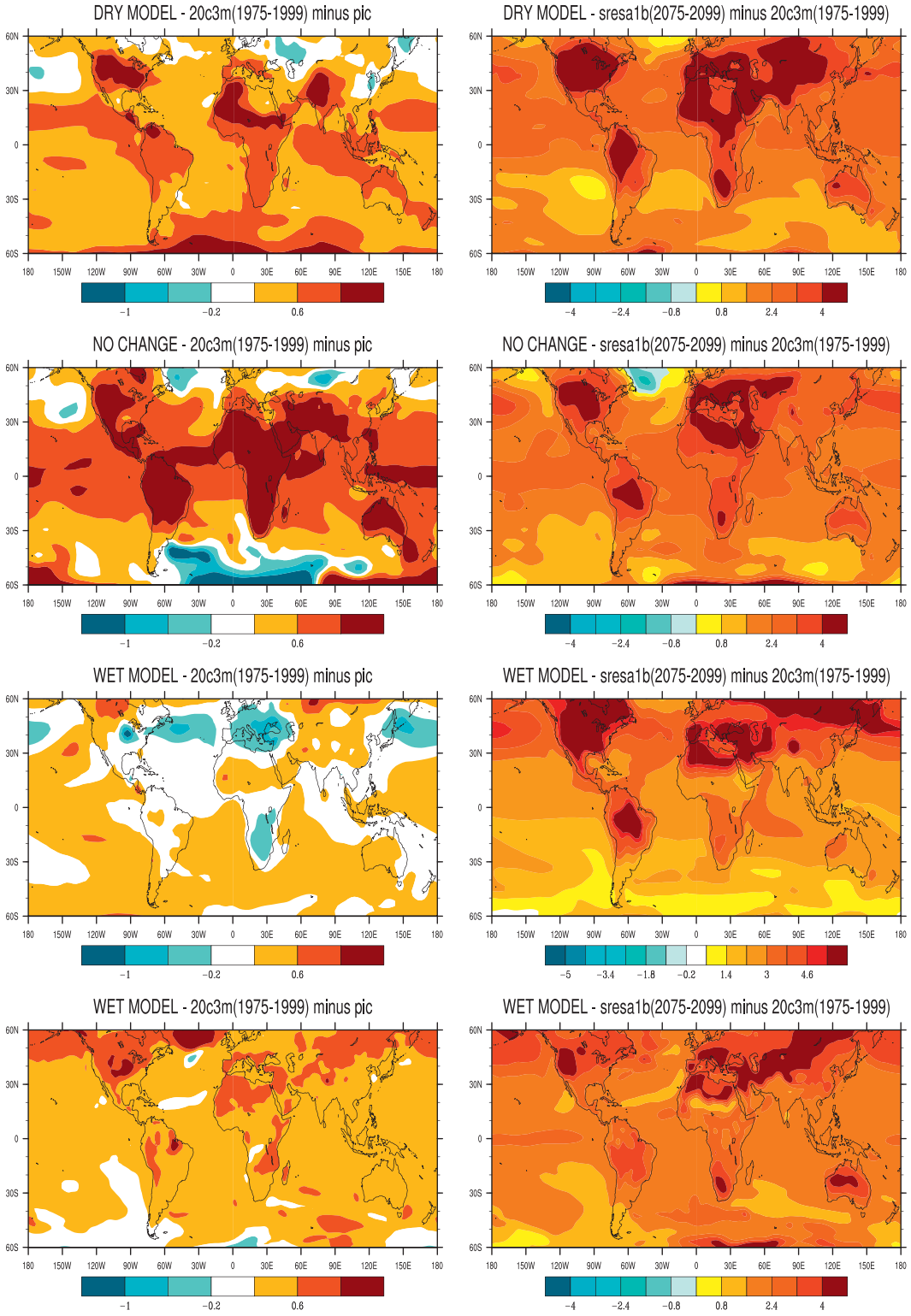

FIG. 1. Differences in surface air temperature (left) between the end of the twentieth century and the preindustrial control and (right) between the end of the twenty-first and the end of the twentieth century. Color scale ranges are between −1° and 1°C on the lhs (the plots of change between end of the twentieth century and preindustrial control) and −4° and 4°C on the rhs (the plots of change between end of the twenty-first and end of the twentieth centuries), except for the third panel on the rhs in which the range is −5°–5°C.

TABLE 1. Spatial correlations of the difference pattern in surface air temperature between the end of the twenty-first century and the end of the twentieth century and the difference pattern between the end of the twentieth century and the preindustrial control, i.e., between the patterns on the lhs and rhs of Fig. 1. See text for details.

	GFDL CM2.0	CNRM-CM3	MIROC(medres)	NCAR CCSM3
90°S–90°N	0.73	0.46	0.21	0.83
60°S–60°N	0.73	0.62	0.11	0.85
30°S–30°N	0.91	0.91	0.38	0.94

both the energy and water cycles, Neelin and Held (1987) combine the energy (T) and water (q) equations to derive an equation for moist static energy (MSE), $m = gz + c_pT + Lq$, where z is geopotential height, T is temperature, q is specific humidity, g is gravity, c_p is the specific heat at constant pressure, and L is the latent heat of evaporation:

$$\partial_t m + \mathbf{\nabla} \cdot m\mathbf{v} + \partial_p m\omega = g\partial_p F, \tag{1}$$

where F is the total energy flux.

In equilibrium, that is, when the first term on the lhs can be ignored, this equation relates changes in dynamics (i.e., in $\mathbf{v}$ and ω) or thermodynamics (i.e., in q), on the lhs, with changes in the net energy budget, on the rhs. Neelin and collaborators (Neelin et al. 2003; Chou and Neelin 2003, 2004; Chou et al. 2009) exploit this formulation to describe the contributions from changes in humidity or in horizontal gradients of humidity, in $\mathbf{\nabla} \cdot m\mathbf{v}$, such as the ''rich get richer'' mechanism whereby wet, deep convective regions are projected to become wetter in a warmer, moister world and the ''upped ante'' mechanism whereby the core regions of deep convection are projected to become wetter at the expense of their margins, which cannot import moisture as effectively.

This study relates changes in moist static energy, in the lhs of Eq. (1), with changes in the net atmospheric energy budget, on the rhs of Eq. (1). Moist static energy and its relation to precipitation change is the focus of the first subsection, while the net surface energy budget and its relation to changes in regional temperature and precipitation is the focus of the second subsection.

a. Precipitation and moist static energy: Local and remote mechanisms of vertical stability change

Figures 2 and 3 display pointwise, or grid box by grid box, regressions of precipitation and moist static energy (MSE) in the twentieth and twenty-first century simulations—near the surface (between the surface and 700 hPa) on the lhs and at upper levels (between 300 and 100 hPa) on the rhs of each figure.

In the twentieth century simulations (Fig. 2) there is coherence among models and between near surface and upper levels. The correlation between precipitation and near-surface MSE is positive all across the Sahel—the swath across Africa at the northern edge of the Northern Hemisphere monsoon climatology, contoured in thin black lines. At the poleward margin of seasonal precipitation the sign of the relationship between precipitation and MSE is determined by the moisture term (Lq) (not shown): above-normal precipitation is associated with above-normal evaporation, to be discussed in greater detail later, hence with a cooler and moister but overall more energetic near-surface layer. Upper-level MSE follows lower-level MSE: the patterns on the rhs of Fig. 2 are weaker but mirror those on the lhs.

The behavior of the wet models does not change in the twenty-first century simulations (Fig. 3, bottom two rows). Precipitation is positively correlated with MSE, with greater amplitude near the surface than at upper levels. In these models, the positive trend in precipitation is accompanied by an increase in near-surface MSE due to the increase in humidity.

The behavior of the dry model especially, but also the model projecting no significant change (Fig. 3, top two rows), is where this picture breaks down. In the dry model, the relationship between precipitation and upper-level MSE changes sign in the entire Northern Hemisphere summer African monsoon region: the negative trend in precipitation is associated with a positive trend in upper-level MSE—the telltale sign of the remote, stabilizing influence of oceanic warming hypothesized by Held et al. (2005) and Giannini et al. (2008). If the trend is removed (not shown), one recovers the same pattern as in Fig. 2, rhs. Near the surface (Fig. 3, top lhs panel) at the poleward margin of seasonal rainfall, the relationship between precipitation and MSE is positive, meaning that a decrease in precipitation is accompanied by a decrease in evaporation and humidity.

These changes are suggestive of vertical stability being set from the bottom up in the case of models projecting a wetter Sahel and from the top down in the case of models projecting a drier Sahel. But how do changes in vertical stability relate to the rhs of Eq. (1), that is, the net surface and atmospheric energy budgets? How do they explain regional change in temperature and rainfall?

b. Mechanisms of regional change in temperature and precipitation

The analysis is linear, based on scatterplots to represent correlation among variables. In Figs. 4–7, green open circles represent points from the preindustrial control (pic), blue filled circles represent points from the

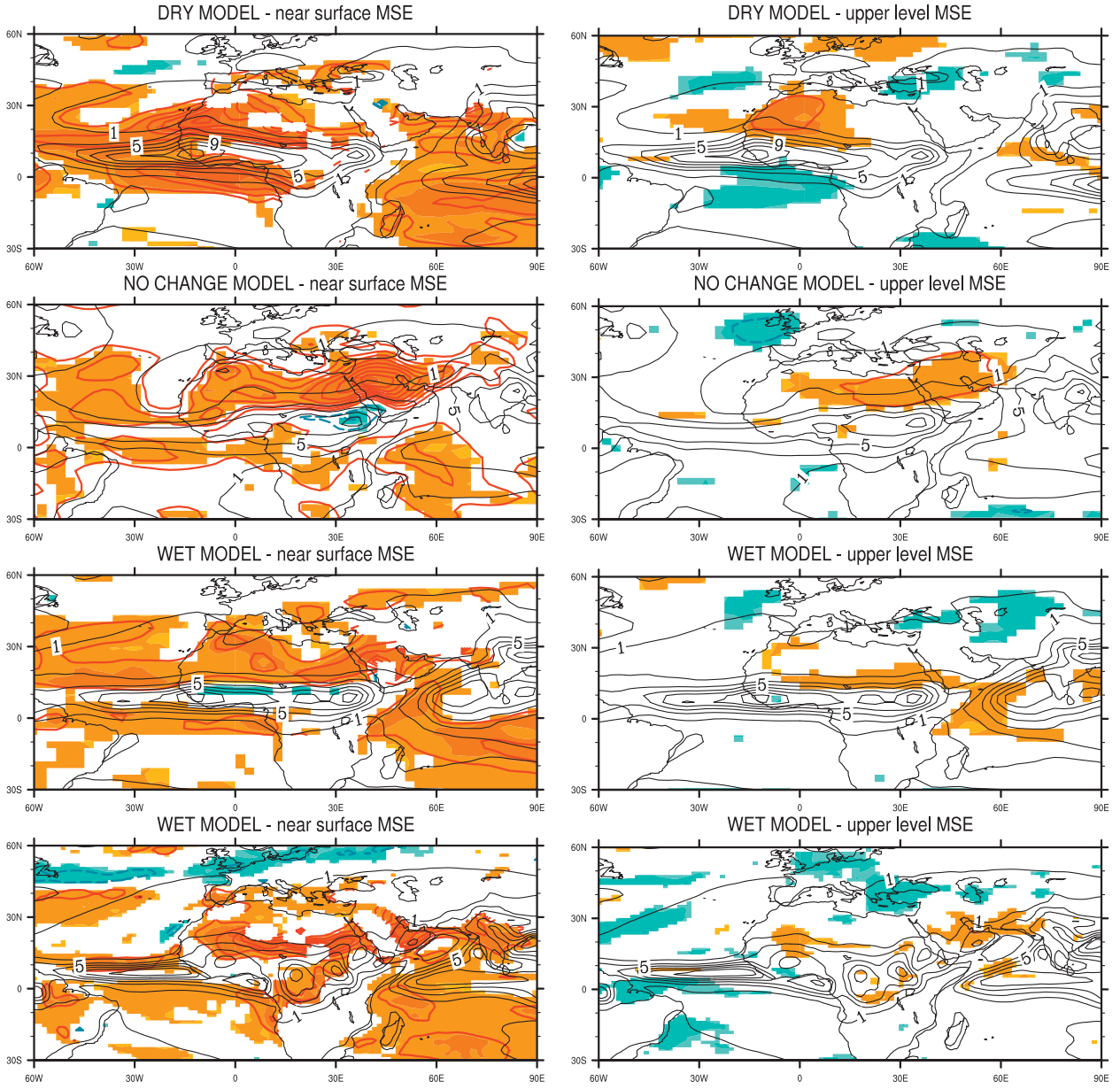

FIG. 2. Pointwise (grid box by grid box) regressions of precipitation and moist static energy in the 20c3m simulations. Color contours (red for positive values, blue for negative values) represent the regression values in units of moist static energy, the presence of shading indicates 95% significance or higher, and thin black contours represent the precipitation climatology, with contours every 2 mm day^{-1}, starting at 1 mm day^{-1}. (left) Moist static energy near the surface, i.e., integrated from the surface to 700 hPa, and (right) moist static energy at upper levels, i.e., integrated between 300 and 100 hPa.

twentieth century simulation (20c3m), and red open squares represent points from scenario A1B (sresa1b). Each point is a spatial average, spanning the Sahel—from 10° to 20°N, 20°W to 40°E—of seasonal mean values for the core monsoon season in Africa north of the equator from July to September. The analysis uses 500 years of pic and up to three ensemble members (when available) of 20c3m and sresa1b for 1900–99 and 2004–99, respectively. The corresponding correlation values are reported in Tables 2 and 3. In each one of the columns in Figs. 4–7, the top panel is GFDL CM2.0, a model projecting significant future drying; followed by CNRM-CM3, a model projecting no significant change; then the two models projecting a significantly wetter future Sahel—MIROC(medres) and NCAR CCSM3.

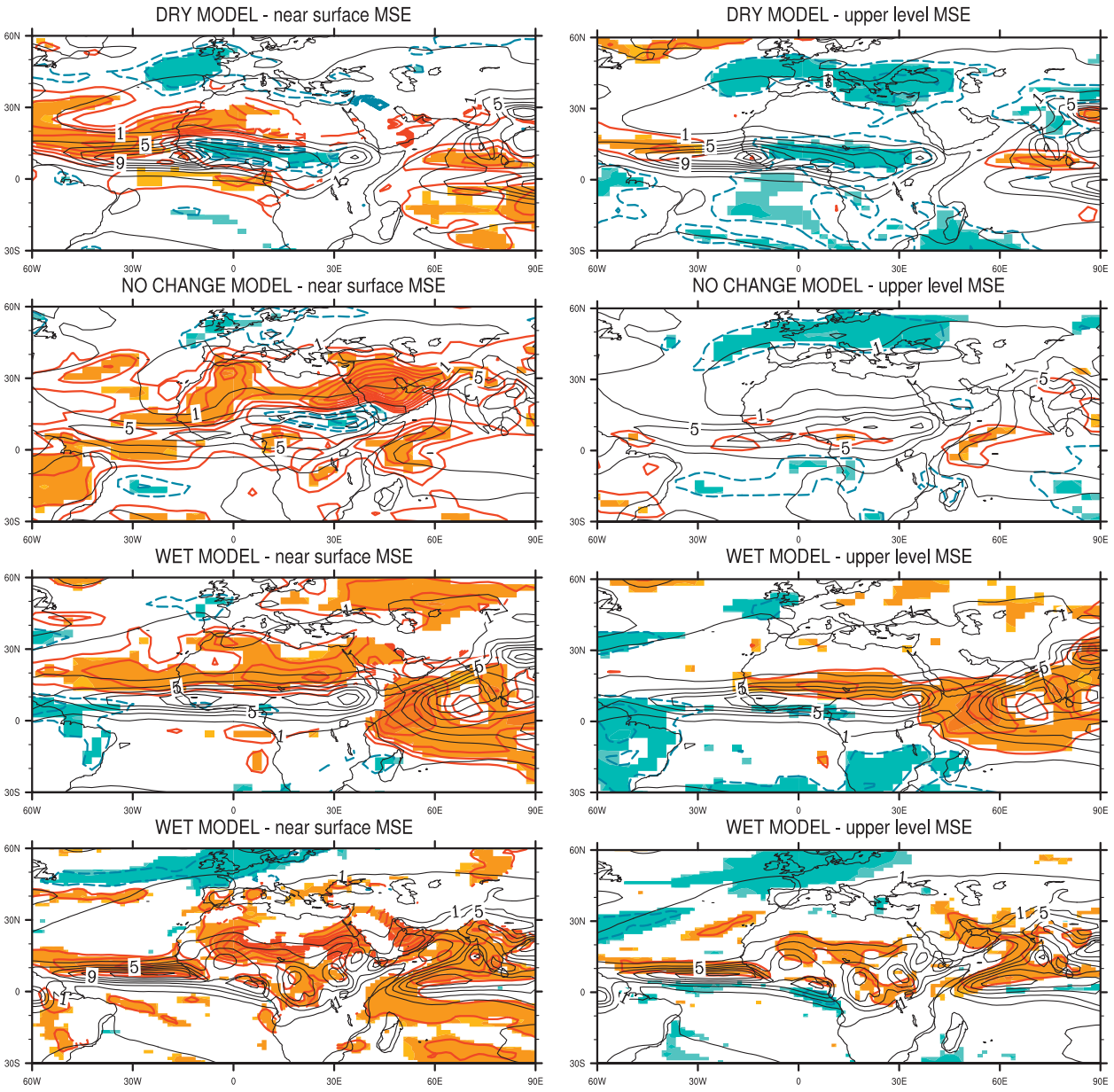

FIG. 3. As in Fig. 2 but for the sresa1b simulations.

1) THE RELATION BETWEEN TEMPERATURE CHANGE, EVAPORATION, AND PRECIPITATION

The scatterplots in Fig. 4 sample the relationship between surface air temperature and evaporation (lhs), and between surface air temperature and precipitation (rhs). Two features are apparent in these plots. One describes the year-to-year variability, prominent in pic and in 20c3m, the historical simulations. The other describes the effect of long-term warming, in sresa1b, which can be generally decomposed into a part parallel, or consistent with the historical relationship, and in a part orthogonal, or independent of it. The historical simulations in Fig. 4 are dominated by negative linear relationships between temperature on one side and evaporation and precipitation on the other. Assuming that enough energy is available at the surface to evaporate soil moisture—the next subsection will return to the role of net surface radiation—abundant rainfall is a precursor of above-average evaporation, which leads to cooling of the surface and near-surface air; that is, the energy available is used on the phase

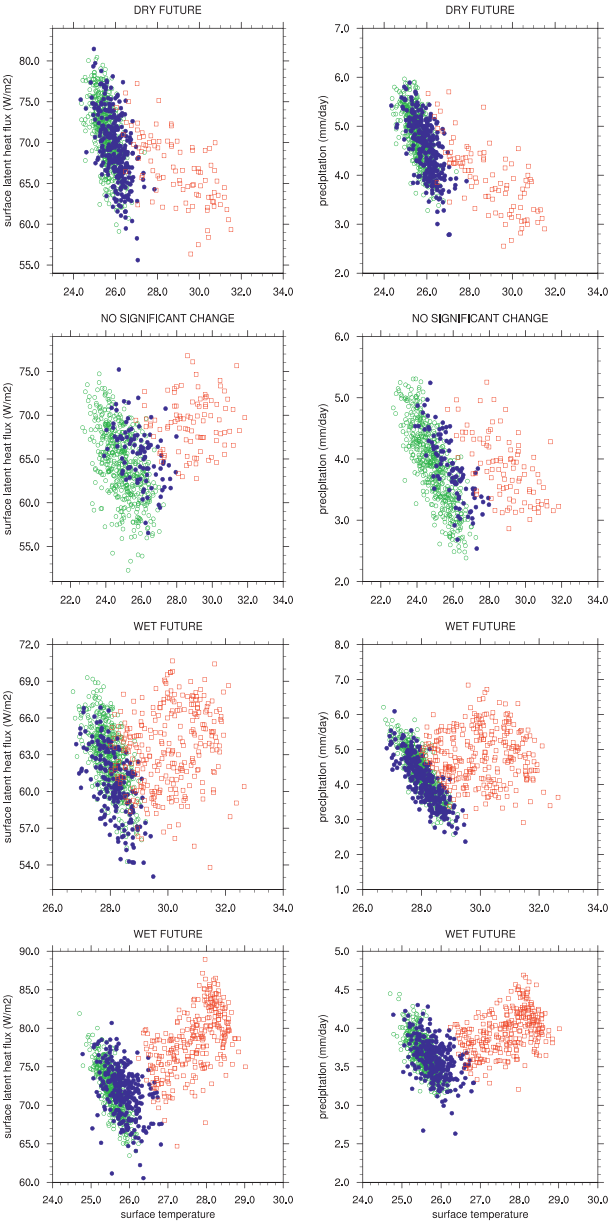

FIG. 4. Scatterplots of (left) temperature and net latent heat flux at the surface, or evaporation, and (right) temperature and precipitation. Green open circles represent points in pic, blue filled circles represent points in 20c3m, and red squares represent points in sresa1b.

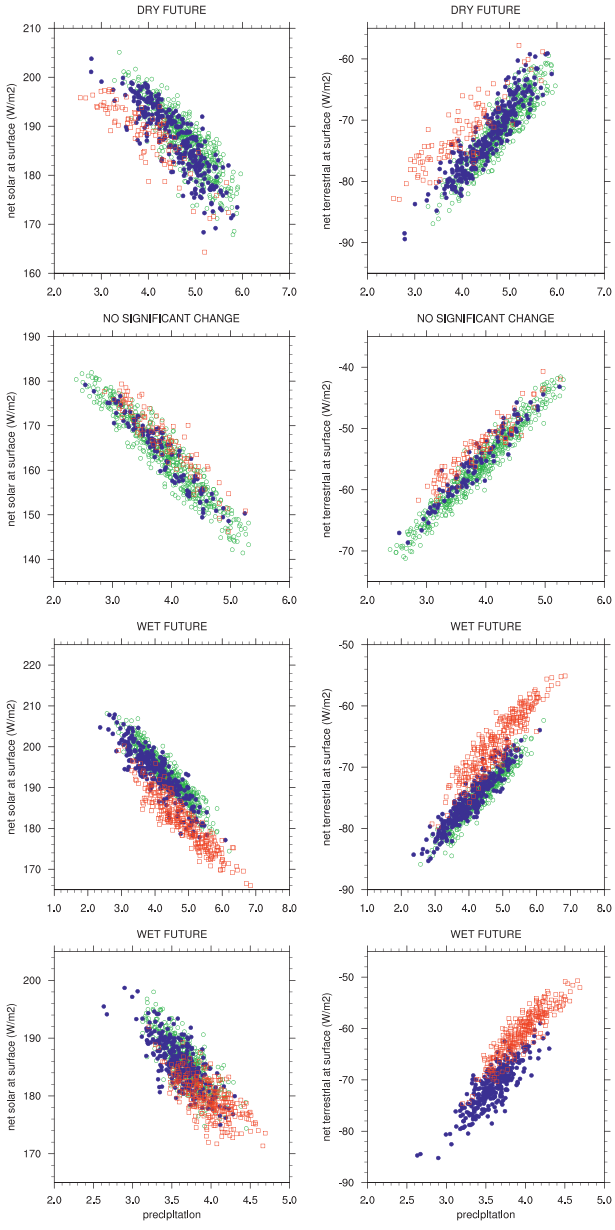

FIG. 5. As in Fig. 4 but of (left) precipitation and net solar radiation at the surface and (right) precipitation and net terrestrial radiation at the surface.

transition of water from liquid to gas rather than on warming. Conversely, below-average precipitation is followed by reduced evaporation and warming.

If one were to base expectation of future behavior on understanding of past behavior, then one would be tempted to infer that the future local change in rainfall could contribute to the change in temperature—if rainfall increased locally in a warmer world, the cooling associated with increased evaporation would temper the global warming signal. If rainfall decreased, it would accentuate the warming signal. The twenty-first-century scatter does, indeed, bear out this expectation. The most notable feature in all panels in Fig. 4 is the rightward translation of points toward warmer temperatures—an indication that there is a significant component to the warming that cannot be predicted from linear extrapolation of the historical fit between temperature and precipitation or evaporation. Presumably, this is the

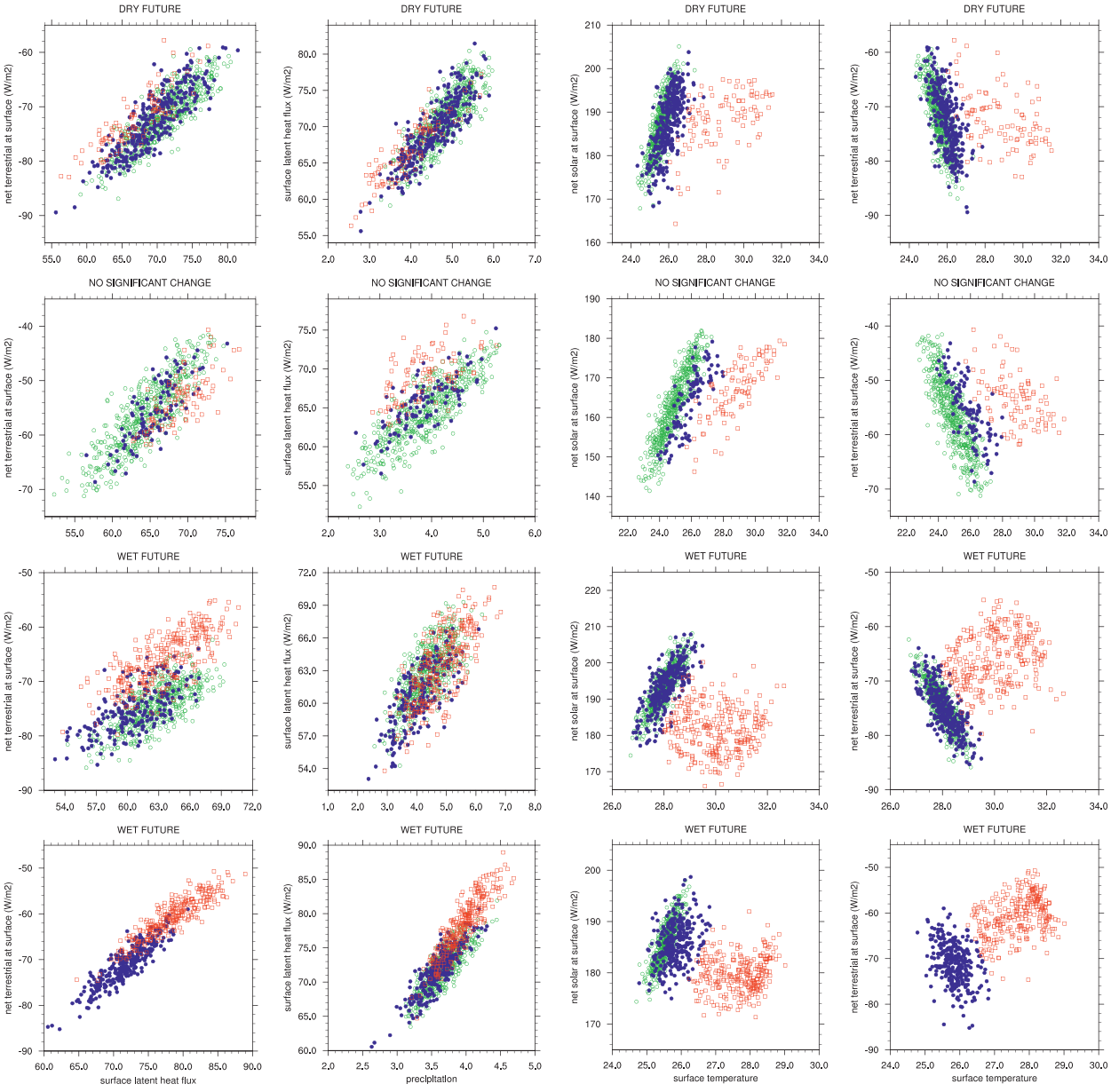

FIG. 6. As in Fig. 4, but of (left) evaporation and net terrestrial radiation at the surface and (right) precipitation and evaporation. Note that in (bottom left) model output of net terrestrial radiation in pic is missing.

FIG. 7. As in Fig. 4, but of (left) air temperature and net solar radiation at the surface and (right) air temperature and net terrestrial radiation at the surface.

component due to the direct radiative effect of greenhouse gases. This translation is largely perpendicular, or orthogonal, to the negative slope delineated by the historical simulations, which I interpret as independence of the physical processes represented. However, the negative relationship between temperature and evaporation or precipitation can still be recognized, in all models, in the year-to-year variations superimposed on the long-term trend—as if the sresa1b points gradually translated the historical relationship toward a warmer basic state.

Nevertheless, there are differences among models. The model in the top panels of Fig. 4 is one "end member": while warming perpendicular to the change in evaporation or precipitation is not negligible, future trends are more in line with the historical scatter than in other models, especially in the temperature–precipitation panel, where data points shift toward the lower right corner, that is, toward drier, warmer conditions. The model in

TABLE 2. Correlation values *r* relative to the panels in Figs. 4 and 5: tas is surface air temperature, pr is precipitation, hls is surface latent heat flux, rns is net solar radiation at the surface, and rnt is net terrestrial radiation at the surface.

	r(tas, pr)	*r*(tas, hls)	*r*(pr, rns-rnt)	*r*(pr, rns-rnt)
GFDL CM2.0				
pic	−0.66	−0.58	−0.85	0.91
20c3m	−0.65	−0.56	−0.85	0.92
sresa1b	−0.71	−0.65	−0.84	0.87
CNRM-CM3				
pic	−0.80	−0.53	−0.95	0.98
20c3m	−0.76	−0.45	−0.95	0.96
sresa1b	−0.59	0.09	−0.93	0.94
MIROC(medres)				
pic	−0.84	−0.62	−0.94	0.95
20c3m	−0.81	−0.59	−0.88	0.93
sresa1b	−0.04	0.19	−0.92	0.92
NCAR CCSM3				
pic	−0.69	−0.76	−0.77	
20c3m	−0.42	−0.41	−0.75	0.84
sresa1b	0.40	0.52	−0.66	0.90

TABLE 3. Correlation values relative to the panels in Figs. 6 and 7: tas is surface air temperature, pr is precipitation, hls is surface latent heat flux, rns is net solar radiation at the surface, and rnt is net terrestrial radiation at the surface.

	r(hls, rnt)	*r*(pr, hls)	*r*(tas, rns)	*r*(tas, rnt)
GFDL CM2.0				
pic	0.87	0.83	0.82	−0.76
20c3m	0.87	0.87	0.68	−0.63
sresa1b	0.86	0.89	0.52	−0.45
CNRM-CM3				
pic	0.85	0.84	0.90	−0.83
20c3m	0.80	0.76	0.83	−0.73
sresa1b	0.71	0.57	0.78	−0.46
MIROC(medres)				
pic	0.71	0.71	0.85	−0.84
20c3m	0.66	0.74	0.73	−0.75
sresa1b	0.76	0.73	−0.02	0.23
NCAR CCSM3				
pic	—	—	0.83	—
20c3m	0.89	0.88	0.39	−0.37
sresa1b	0.90	0.89	0.15	0.35

the bottom panels of Fig. 4 is the other end member: the long-term warming trend dominates and is entirely independent of changes in evaporation or precipitation.

2) THE RELATION BETWEEN PRECIPITATION AND NET SURFACE RADIATION

Next, the relationship is diagnosed between precipitation, evaporation, and terms in the net surface radiative balance: the net solar (shortwave) and terrestrial (longwave) radiation, taken to be positive into the surface.

The relationships between precipitation and net solar radiation and precipitation and net terrestrial radiation tease out the role of clouds in connecting the energy and water cycles—they are displayed in Fig. 5 and quantified in the rightmost two columns of Table 2. Cloud cover increases with increased precipitation; hence, precipitation and solar radiation are negatively correlated (Fig. 5, lhs), because cloud cover reduces the incoming solar radiation at the surface, and precipitation and terrestrial radiation are positively correlated (Fig. 5, rhs), because cloud cover increases the proportion of outgoing terrestrial radiation that is trapped.

The scatterplots bear out these expected relationships in the historical simulations. In the twenty-first century simulations, the changes are in part consistent with these relationships, which are in part orthogonal. In the top two rows of Fig. 5, that is, in the models projecting either a drier Sahel or no significant change, the changes are consistently orthogonal to the historical relationships, meaning that changes in net radiation at the surface, especially the change in net terrestrial radiation (on the rhs), and changes in precipitation are independent of each other. In the bottom two rows, twenty-first century change is consistent, or in line, with the historical relationship: as rainfall increases, net solar radiation decreases, while net terrestrial radiation increases. It is this last relationship, between net terrestrial radiation and precipitation in the model in the bottom row, that permits an interpretation linking the direct radiative effect of greenhouse gases to precipitation change: if the anthropogenic influence on net terrestrial radiation is the origin of change—after all, this is the premier perturbation to the climate system—then it is such forcing that causes an increase in precipitation and cloud cover, and a consequent decrease in net solar radiation, in ways detailed in the next subsection.

3) THE ANTHROPOGENIC GREENHOUSE EFFECT, EVAPORATION, AND PRECIPITATION

How this happens becomes clear when one considers the relationship between evaporation and net terrestrial radiation at the surface (in the lhs of Fig. 6). In the historical simulations, this is a positive correlation. In the semiarid Sahel it is the net terrestrial component that dominates the interaction between clouds and net radiation at the surface (not shown) and allows for evaporation to be enhanced as a consequence of increased rainfall and cloud cover, despite the concurrent cloud-mediated decrease in net solar radiation. In all models there is a significant component of the future change that is consistent (parallel) with historical behavior, but

this is clearest in one of two models projecting a wetter Sahel—that in the bottom row. Because the change in net terrestrial radiation originates in the change in greenhouse gas concentrations, this change can be interpreted as the origin of a causal chain: it is the local change in net terrestrial radiation at the surface that causes a change, first in evaporation and then in precipitation. Conversely, the change in the model projecting a drier Sahel (in the top row of Fig. 6, lhs) is perpendicular to the historical relationship. Consistent with those in Fig. 5, it is again representative of independence between the change in evaporation and that in net terrestrial radiation in the twenty-first century.

Interpretation of these relationships can be constructed as either one of two causal chains of interrelated processes: 1) a (negative) change in precipitation remotely forced by warming of the ocean causes a consistent change in net surface solar radiation and evaporation or 2) a local terrestrial change in evaporation, caused by a change in net surface radiation induced by the anthropogenic increase in greenhouse gases, forces a (positive) change in precipitation.

Thus, the two end members in the top and bottom rows on the rhs of Fig. 6, which depicts the relationship between precipitation and evaporation, represent oppositely directed causality chains with opposite outcomes. The positive relation between precipitation and evaporation that characterizes historical simulations in all models is translated either downward toward dry (top panel) or upward toward wet (bottom panel). In the top panel, representing models that project a drier future Sahel, the remotely forced decrease in precipitation causes a decrease in evaporation. In the bottom panel, representing the models that project a wetter future, the direct effect of an anthropogenic increase in greenhouse gases forces an increase in net terrestrial radiation into the surface, which causes an increase in evaporation that leads to an increase in precipitation. Intermediate outcomes should be interpreted as a combination of these two processes. For example, the model in the second row from the top projects no change in precipitation in conjunction with an insignificant increase in evaporation. Neither of the two processes described, remote or local, dominates. Remote oceanic forcing shifts the region to drying, but at the same time increased net terrestrial radiation favors increased evaporation—hence the uncertain outcome.

4) MECHANISMS OF TEMPERATURE CHANGE

Finally, Fig. 7 displays the contributions of the net solar (lhs) and net terrestrial (rhs) components of surface radiation to temperature change, quantified in the two rightmost columns of Table 3. In the historical simulations, pic and 20c3m, warming is explained by an increase in net solar rather than in net terrestrial radiation at the surface: the correlation is positive in the lhs scatter (third column from left in Table 3) and negative in the rhs (fourth column from left in Table 3). These relationships are consistent with warming being brought about simultaneously by below-average cloud cover and below-average evaporation, both consequences of below-average precipitation, and it is, indeed, reflected in significant negative correlation values between temperature and precipitation (Table 2, leftmost column). The warming in the twenty-first century simulations is explained by changes in net surface solar radiation in the models in the two top rows in Fig. 7 and by changes in net surface terrestrial radiation in the models in the two bottom rows in Fig. 7. Note that, in both cases, future change is largely orthogonal to past relationship, especially so in the models in the two bottom rows.

c. *Budgets of energy and water*

The analysis so far has focused on mechanisms that can initiate a change and in this respect can be directly tied to an enhanced greenhouse effect. For this reason the focus has been primarily on local processes. However, one can also imagine that the atmospheric circulation adjusts to these changes in a way that reinforces them. For example, once precipitation is reduced through the remote top-down mechanism described, which makes the atmosphere more stable or, equivalently, increases subsidence, the convergent circulation is consistently weakened, and a decrease in moisture convergence further reduces precipitation. Conversely, in the case of an increase in evaporation and precipitation associated with the local bottom-up mechanism, upward motion is followed by near-surface convergence and enhancement of precipitation. This is indeed the case in the models projecting a significant change, dry or wet. Figure 8 displays the scatterplots of the net water and energy balances in the Sahel. These are measured respectively by the balance of precipitation and evaporation ($P - E$) on the X axis and by the net atmospheric energy balance—the difference between net energy at the surface and at the top of the atmosphere—on the Y axis. In the dry model the increase in net atmospheric energy goes along with a decrease in $P - E$, that is, in moisture convergence. In the wet models the same increase in net atmospheric energy goes along with an increase in $P - E$. The model projecting insignificant change is characterized by insignificant changes in either variable. Perhaps in this case negative feedbacks are at play—for example, an increase in humidity that could in itself bring about an increase in moisture convergence if the circulation stayed the same is counteracted by a weakening of the circulation.

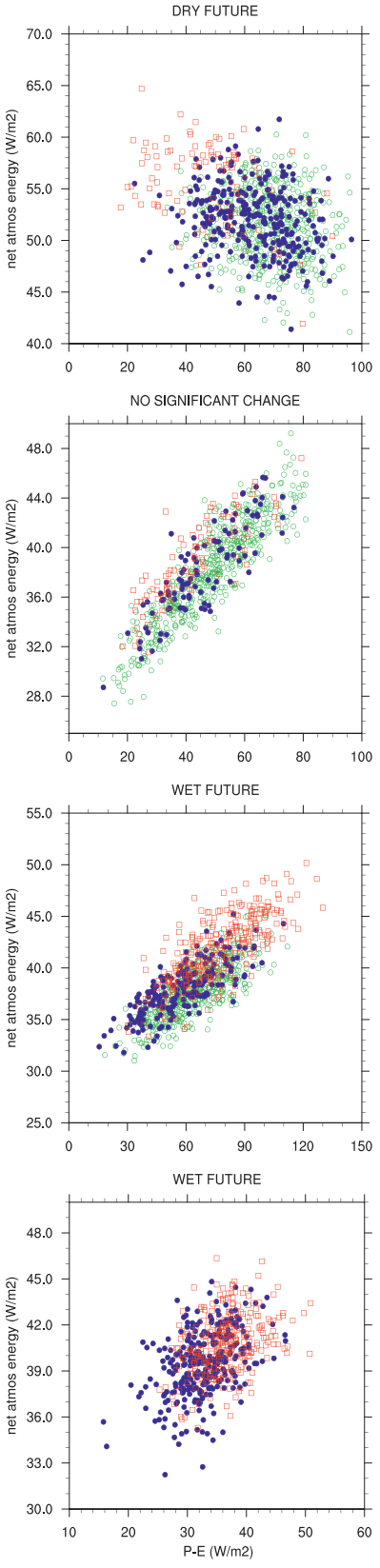

FIG. 8. As in Fig. 4 but of $P - E$ and net atmospheric energy.

5. Discussion and conclusions

This analysis breaks down the steps in two competing pathways of climate change in the Sahel—one remotely forced from the ocean and the other local and directly related to the radiative effect of anthropogenic greenhouse gases on the net surface energy balance over land.

In one pathway, twenty-first century changes in precipitation and stability, depicted in Figs. 2 and 3, are dictated by oceanic warming, which imposes stability from the top down and favors deep convection and precipitation over water where moisture is readily available, at the expense of land. The reduction in precipitation over land is followed by a reduction in evaporation and by an increase in net solar radiation at the surface associated with reduced cloud cover, which add up to explain the local warming. The crucial relationship symbolizing this pathway, taken by the model displayed in the top panels, is that depicted in Fig. 4, between temperature and precipitation. For this model, this is the most consistent between historical and twenty-first-century simulations.

In the other pathway, an increase in net terrestrial radiation into the land surface, a direct effect of the increase in anthropogenic greenhouse gases, increases evaporation, affecting vertical stability locally from the bottom up. Local instability fuels deep convection and near-surface moisture convergence—a stronger monsoonal inflow—and favors an increase in precipitation, The same increase in net terrestrial radiation, triggered by anthropogenic greenhouse gases and enhanced by the increase in water vapor in the boundary layer, explains surface warming. The crucial relationship in this pathway, taken by the model displayed in the bottom panels depicted in Fig. 6 (lhs), is between evaporation and net terrestrial radiation, which is again coherent between historical and twenty-first century simulations.

The recent studies of Held et al. (2005) and Haarsma et al. (2005), which paint opposing pictures of future climate change in the Sahel, can be made sense of in this framework. In Held et al. (2005), a simple 2 K warming of the global oceans leads to drying of the Sahel in two out of three models analyzed, which include the ''dry'' end member here. In these models the remote oceanic forcing dominates. The third model in Held et al. (2005) is an updated version of that used by Haarsma et al. (2005) to characterize future climate change in the Sahel as a strengthening of the monsoonal circulation associated with an increase in the land–ocean temperature contrast. This is one of two ''wet'' end members here. In this model the local forcing of an enhanced greenhouse effect dominates. In models that do not project a significant change, neither of the two processes, remote or

local, dominates; hence these mechanisms end up partially canceling out each other.

It is worthwhile to reconsider past studies in light of these findings. Claussen et al. (2003) argued that the early mid-Holocene humid period in northern Africa may not be an appropriate analog for anthropogenic climate change. To the extent that net solar and net terrestrial radiation at the surface interact in opposite ways with clouds and the water cycle, this study lends support to that contention. An external increase in net solar radiation associated with variation in orbital parameters, if it led to a stronger monsoon and an increase in precipitation, would be naturally limited by the concomitant increase in clouds in ways that an increase in net terrestrial radiation would not—unless the net terrestrial radiation at the surface took up the slack and started to contribute significantly to the net surface energy budget, and to evaporation, in a positive feedback loop.

Yang et al. (2003) separately consider the direct effect of an increase in greenhouse gases and the indirect effect, through oceanic warming, on the hydrological cycle and reach conclusions that are only apparently at odds with those discussed here. In their simulations an increase in CO_2 leads to a more stable atmosphere, hence a weaker hydrological cycle, while an increase in SST leads to a more unstable atmosphere, hence a stronger hydrological cycle. Presumably these results depend on whether models place greater control on vertical stability at the top or bottom of the atmosphere.

Biasutti and Giannini (2006) suggest that the incoherence of twenty-first century projections of Sahel rainfall, in the face of their coherence in the representation of late-twentieth century drying, may have to do with the greater weight carried by the presence of sulfate aerosols in twentieth century simulations. In the present framework the presence of sulfate aerosols may affect Sahel rainfall differently in these two different categories of models, with the same end result. In one category, aerosols affect Sahel rainfall indirectly, through the interhemispheric gradient in sea surface temperature that they set up (Rotstayn and Lohmann 2002)—sulfate aerosols are more abundant closer to the source, that is, in the Northern Hemisphere; hence warming of the Northern Hemisphere oceans is muted compared to the Southern Hemisphere, a condition known to be unfavorable for abundant rainfall in the Sahel (Lamb 1978; Folland et al. 1986). In the other, they affect Sahel rainfall directly through the net surface energy balance over land: their increased concentration throughout the twentieth century reduced net solar radiation, hence evaporation over land. In either case, aerosols conspire to reduce precipitation.

Paeth et al. (2009) find high sensitivity to local changes in land use in regional model simulations forced with a global climate model that predicts no significant change in rainfall in the Sahel according to Biasutti and Giannini (2006), that is, Max Planck Institute (MPI) ECHAM5. In their Fig. 5 they show small changes of either sign in rainfall across the Sahel when their regional model simulations are driven by the global model in the sresa1b scenario, in contrast to a large decrease when projections of land use change are added. Given that the forcing global model alone is producing no significant change, it is reasonable to explain this behavior as one where local processes dominate, only of sign opposite to those discussed here. In this case the Charney feedback applies (Charney 1975; Otterman 1974): baring of soil reduces the net radiation at the surface, hence evaporation and moist static energy, and brings about drier and warmer conditions.

Change in the model projecting a drier Sahel is drastic, given the impact that the persistence of drought in the 1970s and 1980s, a drop of the order of 10%–20% in seasonal rainfall totals, has already had on the system. But, it is closer in its physical basis to the change that the Sahel has already witnessed: oceanic warming leads to drying—barred the confounding factor brought about by Atlantic multidecadal variability. Change in the models projecting a wetter Sahel is more extreme, though physically plausible, in that it shifts the balance from ocean to land—from an indirect effect of anthropogenic warming on SST to its direct impact on evaporation over land. At present, there is no way to discern whether in the balance the future of the climate system is going to be different from that experienced over the twentieth century instrumental record. Certainly, closer monitoring of trends in terms in the net surface energy balance, and in their interaction with clouds and the water cycle, will be only a necessary first step to discriminate among the scenarios of future change but one that may prove useful to our understanding of impacts on the environment and societies in the region.

Acknowledgments. AG acknowledges the modeling groups, the Program for Climate Model Diagnosis and Intercomparison (PCMDI) and the Working Group on Coupled Modelling (WGCM) of the World Climate Research Programme (WCRP) for their roles in making available the WCRP CMIP3 multimodel dataset. Support of this dataset is provided by the Office of Science, U.S. Department of Energy. AG wishes to thank Beate Liepert, Madeleine Thomson, Michela Biasutti, Adam Sobel, Isaac Held, Yochanan Kushnir, Mingfang Ting, and Lisa Goddard for the knowledge, intellectual and practical, shared over the past 5 years, and the National

Oceanic and Atmospheric Administration for its financial support, through Grant NA07GP0213.

REFERENCES

Adeel, Z., U. Safriel, D. Niemeijer, and R. White, 2005: Ecosystems and human well-being: Desertification synthesis. World Resources Institute, Washington, DC, 26 pp. [Available online at http://www.millenniumassessment.org/documents/document.355.aspx.pdf.]

Bader, J., and M. Latif, 2003: The impact of decadal-scale Indian Ocean sea surface temperature anomalies on Sahelian rainfall and the North Atlantic Oscillation. *Geophys. Res. Lett.,* **30,** 2169, doi:10.1029/2003GL018426.

Barnett, T. P., D. W. Pierce, K. M. AchutaRao, P. J. Gleicker, B. D. Santer, J. M. Gregory, and W. M. Washington, 2005: Penetration of human-induced warming into the world's oceans. *Science,* **309,** 284–287.

Biasutti, M., and A. Giannini, 2006: Robust Sahel drying in response to late 20th century forcings. *Geophys. Res. Lett.,* **33,** L11706, doi:10.1029/2006GL026067.

——, I. M. Held, A. H. Sobel, and A. Giannini, 2008: SST forcings and Sahel rainfall variability in simulations of twentieth and twenty-first centuries. *J. Climate,* **21,** 3471–3486.

Charney, J. G., 1975: Dynamics of deserts and drought in the Sahel. *Quart. J. Roy. Meteor. Soc.,* **101,** 193–202.

Chiang, J. C. H., and A. H. Sobel, 2002: Tropical tropospheric temperature variations caused by ENSO and their influence on the remote tropical climate. *J. Climate,* **15,** 2616–2631.

Chou, C., and J. D. Neelin, 2003: Mechanisms limiting the northward extent of the northern summer monsoons over North America, Asia, and Africa. *J. Climate,* **16,** 406–425.

——, and ——, 2004: Mechanisms of global warming impacts on regional tropical precipitation. *J. Climate,* **17,** 2688–2701.

——, ——, and H. Su, 2001: Ocean-atmosphere-land feedbacks in an idealized monsoon. *Quart. J. Roy. Meteor. Soc.,* **127,** 1869–1891.

——, ——, C.-A. Chen, and J.-Y. Tu, 2009: Evaluating the rich-get-richer mechanism in tropical precipitation change under global warming. *J. Climate,* **22,** 1982–2005.

Christensen, J. H., and Coauthors, 2007: Regional climate projections. *Climate Change 2007: The Physical Science Basis,* S. Solomon et al., Eds., Cambridge University Press, 847–940.

Claussen, M., V. Brovkin, A. Ganopolski, C. Kubatzki, and V. Petoukhov, 2003: Climate change in northern Africa: The past is not the future. *Climatic Change,* **57,** 99–118.

Cook, K. H., and E. K. Vizy, 2006: Coupled model simulations of the West African monsoon system: Twentieth- and twenty-first-century simulations. *J. Climate,* **19,** 3681–3703.

Douville, H., D. Salas-Melia, and S. Tyteca, 2006: On the tropical origin of uncertainties in the global land precipitation response to global warming. *Climate Dyn.,* **26,** 367–385.

Folland, C. K., T. N. Palmer, and D. E. Parker, 1986: Sahel rainfall and worldwide sea temperatures, 1901–85. *Nature,* **320,** 602–607.

Giannini, A., R. Saravanan, and P. Chang, 2003: Oceanic forcing of Sahel rainfall on interannual to interdecadal time scales. *Science,* **302,** 1027–1030, doi:10.1126/science.1089357.

——, M. Biasutti, I. M. Held, and A. H. Sobel, 2008: A global perspective on African climate. *Climatic Change,* **90,** 359–383, doi:10.1007/s10584-008-9396-y.

Haarsma, R. J., F. Selten, N. Weber, and M. Kliphuis, 2005: Sahel rainfall variability and response to greenhouse warming. *Geophys. Res. Lett.,* **32,** L17702, doi:10.1029/2005GL023232.

Hagos, S. M., and K. H. Cook, 2008: Ocean warming and late-twentieth-century Sahel drought and recovery. *J. Climate,* **21,** 3797–3814.

Held, I. M., T. L. Delworth, J. Lu, K. Findell, and T. R. Knutson, 2005: Simulation of Sahel drought in the 20th and 21st centuries. *Proc. Natl. Acad. Sci. USA,* **102,** 17 891–17 896, doi:10.1073/pnas.0509057102.

Hoerling, M. P., J. W. Hurrell, J. Eischeid, and A. S. Phillips, 2006: Detection and attribution of twentieth century northern and southern African monsoon change. *J. Climate,* **19,** 3989–4008.

Knight, J. R., C. K. Folland, and A. A. Scaife, 2006: Climate impacts of the Atlantic Multidecadal Oscillation. *Geophys. Res. Lett.,* **33,** L17706, doi:10.1029/2006GL026242.

Lamb, P. J., 1978: Case studies of tropical Atlantic surface circulation patterns during recent sub-Saharan weather anomalies: 1967 and 1968. *Mon. Wea. Rev.,* **106,** 482–491.

Levitus, S., J. I. Antonov, T. P. Boyer, and C. Stephens, 2000: Warming of the world ocean. *Science,* **287,** 2225–2229.

Liepert, B. G., J. Feichter, U. Lohmann, and E. Roeckner, 2004: Can aerosols spin down the water cycle in a warmer and moister world? *Geophys. Res. Lett.,* **31,** L06207, doi:10.1029/2003GL019060.

Lu, J., and T. L. Delworth, 2005: Oceanic forcing of late 20th century Sahel drought. *Geophys. Res. Lett.,* **32,** L22706, doi:10.1029/2005GL023316.

Meehl, G. A., C. Covey, T. Delworth, M. Latif, B. McAvaney, J. F. B. Mitchell, R. J. Stouffer, and K. Taylor, 2007a: The WCRP CMIP3 multimodel dataset: A new era in climate change research. *Bull. Amer. Meteor. Soc.,* **88,** 1383–1394.

——, and Coauthors, 2007b: Global climate projections. *Climate Change 2007: The Physical Science Basis,* S. Solomon et al., Eds., Cambridge University Press, 747–846.

Neelin, J. D., and I. M. Held, 1987: Modeling tropical convergence based on the moist static energy budget. *Mon. Wea. Rev.,* **115,** 3–12.

——, C. Chou, and H. Su, 2003: Tropical drought regions in global warming and El Niño teleconnections. *Geophys. Res. Lett.,* **30,** 2275, doi:10.1029/2003GL018625.

Otterman, J., 1974: Baring high-albedo soils by overgrazing: A hypothesized desertification mechanism. *Science,* **186,** 531–533.

Paeth, H., K. Born, R. Girmes, R. Podzun, and D. Jacob, 2009: Regional climate change in tropical and northern Africa due to greenhouse forcing and land use changes. *J. Climate,* **22,** 114–132.

Rotstayn, L., and U. Lohmann, 2002: Tropical rainfall trends and the indirect aerosol effect. *J. Climate,* **15,** 2103–2116.

Ting, M., Y. Kushnir, R. Seager, and C. Li, 2009: Forced and internal twentieth-century SST trends in the North Atlantic. *J. Climate,* **22,** 1469–1481.

Trenberth, K. E., A. Dai, R. M. Rasmussen, and D. B. Parsons, 2003: The changing character of precipitation. *Bull. Amer. Meteor. Soc.,* **84,** 1205–1217.

Yang, F., A. Kumar, M. E. Schlesinger, and W. Wang, 2003: Intensity of hydrological cycles in warmer climates. *J. Climate,* **16,** 2419–2423.

Zeng, N., and J. D. Neelin, 1999: A land–atmosphere interaction theory for the tropical deforestation problem. *J. Climate,* **12,** 857–872.